An Analysis of Landsat Thematic Mapper P-Product Internal Geometry and Conformity to Earth Surface Geometry*

N. A. Bryant, A. L. Zobrist, R. E. Walker, and B. Gokhman
Image Processing Applications and Development Section, Observational Systems Division, Jet Propulsion Laboratory, California Institute of Technology, Pasadena, CA 91109

ABSTRACT: Five Landsat-4 and five Landsat-5 Thematic Mapper, precision processed, P-Product, scenes were analysed to determine their geometric integrity and conformance to the earth's surface geometry. The geometric integrity tests performed included: band-to-band registration along a line, line-to-line registration within a swath, swath-to-swath registration, and scene-to-ground control location. Earth's surface geometry tests measured the actual versus projected position of Space Oblique Mercator (SOM) and Universal Transverse Mercator (UTM) processed products using P-tape calibration data and ground control points.

The geometric integrity tests showed TM-5 data to meet or exceed registration accuracies found on the TM-4. No problems were observed in the intraband analysis, and aside from indications of slight misregistration between bands of the primary versus bands of the secondary focal plane, interband registration and swath alignment was well within the specified tolerances. In addition, overall geometric integrity of TM scenes was tested for conformance to ground control. A least-squares fit between the line/sample position and latitude/longitude for selected ground control points in each scene was computed. A root mean square error of between 27.27 and 30.57 meters across entire scenes was observed. This closely approximates the accuracy specifications for the TM. Moreover, a significant portion of the error component may be attributable to the precision of ground control point selection.

The test for assessing conformity of the P-Product data to earth surface geometry revealed problems when using the Space Oblique Mercator projection (SOM). A chi-squared goodness of fit test between projected and observed northing and easting position on a UTM grid for ground control points revealed that the data exceeded the error budget. Subsequent analysis showed that the projected image center data computed from ephemeris information was in error. This creates discontinuous distortions from the actual earth geometry which can be retrieved only by use of a number of somewhat uniformly distributed control points over the scene and the application of a third order mapping function. Avoidance of this problem for the SOM projection can be achieved by the ground processing segment either receiving a more accurate ephemeris by using the GPS (Global Positioning System) or identifying a select number of ground control points within the scene along the particular orbit path of acquisition. The user can avoid this problem by specifying UTM formatted P-data, identifying three or more ground control points in a scene, and computing the offset within the UTM zone.

INTRODUCTION

SINCE THE INITIATION of the Landsat Project and the Thematic Mapper (TM) development, there has been concern over the geometric accuracy criteria. Performance requirements have been defined in terms of end product goals but until recently have not detailed precisely the conditions

under which that accuracy is to be achieved. The Thematic Mapper is a sensor with higher spatial resolution and finer spectral discrimination than any previous National Aeronautics and Space Administration (NASA) satellite system. In order to achieve the higher spatial and spectral resolutions, the TM sensor was designed to image in both forward and reverse mirror sweeps in two separate focal planes. The established Multispectral Scanner (MSS) ground data processing systems required major changes to correct the new data's geometry and radiometry. Scanner imaging systems suffer from con-

tinuous along-track and across-track geometric distortions which can be mitigated by both hardware systems and ground processing software corrections. Both hardware and software have been augmented and changed during the course of the Landsat TM developments to achieve improved geometric accuracy. The changes instituted in spacecraft and sensor hardware to achieve project objectives have required adaptation in ground segment processing algorithms and procedures. The purpose of this research has been to verify the accuracy of the geometric corrections applied and to assess the overall geometric integrity of the data.

BACKGROUND

Understanding of and compensation for geometric positioning errors are important for two reasons. First, there is the need to achieve map projection positioning to determine site location and register ancillary data encoded by latitude/longitude. Second, there is the need to register multiple passes of imagery to develop multitemporal data sets for change detection and crop mensuration. Thus, while it is accepted that the higher spatial resolution of the TM will fulfill object recognition requirements for larger scale maps than the MSS, it has been the object of this research to determine if the TM meets the National Map Accuracy Standards for geometric accuracy at larger scales. As Billingsley (1981) has pointed out, for field boundaries, misregistration causes the borders in a given set of bands to be closer than expected to a given pixel, with the result that the mixed materials in the pixel cause additional pixels to fall outside of the class limits. As a result, minimum field size configuration acceptable for TM analysis may not be as small as originally assumed.

The variety of sensor and spacecraft geometric properties contributing to positional error estimates have been reviewed by Prakash and Beyer (1981). The error budget analyses performed show that the TM systematic geometric error may present problems with pixel-for-pixel registration between acquisitions in level terrain. This may be the case for two reasons: (1) the scanner system geometry is more complex than MSS (i.e., forward and reverse acquisitions), and (2) the smaller Instantaneous Field of View (IFOV) (i.e., 30×30 vs. 57×80 m) presents a high probability of band-to-band misregistration within one scene acquisition and a greater incidence of pixel misalignment between two acquisitions. The degree of misalignment will be mitigated by ground control point processing. The impact of relief and simple elevation upon the projective geometry of scanning systems is well understood. What is not fully appreciated, nor could be adequately examined until flight data became available, is the interaction of horizontal displacement due to interworking of scan angle from nadir, surface relief, and the movement of the nadir track and altitude associated with different acquisitions.

POSITIONAL ACCURACY REQUIREMENTS

Early MSS systems suffered from along-track and across-track geometric distortions which had to be mitigated with ground processing software corrections. Scanline problems caused errors up to 7 pixels per line in some scenes. After corrective processing, root mean square (RMS) vector errors of the digital data were reduced to the 1-pixel target. Bernstein reported an RMS vector error of 60.6 m for the data, while for the 'good' scenes evaluated by Graham and Luebbe (1981), the accuracy of the ground control point (GCP) corrected data varied between one and two pixels. At this level of precision, the digital data met the National Map Accuracy Standards for scales at or above 1:125,000.

When the Thematic Mapper was beng designed, rigorous specifications for the corrected data's geometry were established. Not only were the geometric requirements more stringent than for the MSS, but also the smaller IFOV and the necessary hardware design changes presented more possibilities for interband misregistration and other image geometry problems. A single band was required to be accurate to within 0.5 pixels of true Earth-surface locations at any point over 90 percent of the image. With its 30 m pixel resolution, this figure was equivalent to 15 m on the Earth's surface, or between 4 and 8 times as precise as its MSS predecessor had proven to be. Between-band (interband) registration accuracies were stipulated to be within a 0.3 pixel tolerance (9 m) over 90 percent of the data. The same figure was established for the registration between scenes of different dates (temporal registration) of the same area.

It has been the object of this research to determine the degree to which the TM geometric accuracy criteria have been achieved on Landsat-4 and Landsat-5.

METHODS AND RESULTS

OVERVIEW

For the purposes of this investigation, ten TM scenes were analyzed, five from Landsat-4 and five from Landsat-5. Table 1 summarizes the analysis performed on each scene. Five characteristics related to image geometry were investigated: (1) Single band geometric integrity, with particular regard to mirror-scan swath alignments; (2) The registration between the 30 m resolution bands (bands 1–5, and 7) of the same image; (3) Image to image conformity; (4) Conformance of the images to a ground control; and (5) Conformance of the image projective geometry to a mapped earth geometry.

TESTS OF INTRABAND INTEGRITY AND INTERBAND REGISTRATION

Technique. The band-to-band and line-to-line registration was measured at 100 pixel spacings along a line using the phase correlation image alignment method developed by Kuglin and Hines (1977)

TABLE 1. SUMMARY OF LANDSAT THEMATIC MAPPER SCENES ANALYZED

Location	Scene Id	Date	Analysis Applied
1. Washington, DC	40109-15140	11/02/82	a) A-tape and P-tape line matching within a band b) A-tape and P-tape band-to-band matching in primary and secondary focal plane c) Conformance of P-tape to ground control
2. Harrisburg, PA	40109-15134	11/02/82	a) P-tape band-to-band matching in primary and secondary focal plane b) Conformance of P-tape to ground control c) Conformance of SOM projection to mapped Earth geometry, without GCPs
3. Salton Sea, CA	40149-17444	12/12/82	a) Conformance of P-tape to ground control b) Conformance of SOM projection to mapped Earth geometry, without GCPs
4. Harrisburg, PA	40189-15151	01/21/83	a) P-tape registration to scene 40109-15134, assess relief displacement
5. Northwest Iowa	40040-16321	05/09/82	a) Conformance of P-tape to ground control b) Conformance of P-tape to TM-5 scene 50046-16324
6. Washington, DC	50023-15112	03/24/84	a) A-tape and P-tape line matching within a band b) P-tape band-to-band matching in primary and secondary focal plane
7. Northwest Iowa	50046-16324	04/16/84	a) P-tape band-to-band matching in primary and secondary focal plane b) Conformance of P-tape to TM-4 scene c) Conformance of SOM projection to mapped Earth geometry, without GCPs
8. Harrisburg, PA	50099-15141		a) Comparison of SOM and UTM projections with TIPS GCPs
9. Salton Sea, CA	50203-17462	09/20/84	a) Conformance of SOM projection to mapped Earth geometry, with GCPs
10. Des Moines, IA	50114-16223	07/23/84	a) Comparison of UTM projection with and without GCPs in TIPS processing

and adapted to a one-dimensional FFT correlation technique. Misregistration of swaths on forward and reverse scans of the TM was suspected. If that had been the case, phase correlation of the last line of preceding scan and first line of the subsequent scan would have shown an offset, which could have varied along the line due to nonlinearity of scan velocity with time. A program was developed that allowed sampling of each line of the image in a number of locations (corresponding to ground features) and determined the offset in each location relative to the other line.

The following is a one-dimensional application of an approach suggested by Kuglin and Hines (1977). $g_1(x)$ and $g_2(x)$ is a pair of image lines. One-dimensional discrete Fourier Transforms G_1 and G_2 can be computed and the phase difference $e^j (\phi_1 - \phi_2)$ can be obtained for each frequency f as the phase of the convolution of G_1 and G_2:

$$G_i(f) = |G_i(f)| \times e^{j\phi(f)}, \ (i = 1,2)$$

$$e^{j\phi(f)} = d^{j(\phi_1 - \phi_2)} = \frac{G_1 \times G_2{}^*}{|G_1| \times |G_2|} \quad (1)$$

The function $e^{j\ (f)}$ represents the phase of the cross power spectrum, $G_1 \times G_2{}^*$. The phase correlation function is given by the inverse Fourier Transform:

$$d(x) = F^{-1} (e^{j\phi(f)}) \quad (2)$$

and its maximum $d(x)_{max}$ yields the amount of shift x_{max}.

For the simple case of shifted line $g_2(x) = g_1 (x + L)$, the Fourier shift theorem gives $G_2(f) = G_1(f)e^{j\ 2\pi f_x L}$, so that $e^{j\phi} = e^{-j\pi 2 f_x L}$ and the correlation function is $\beta\ (x - L)$. Thus one can expect to see a sharp symmetrical peak in correlation function in location corresponding to the amount of shift. Due to discrete sampling the exact determination of the shift requires calculation of the correlation function in a few points around the maximum and interpolation to find the position of the peak. Since the peak is expected to be symmetric, quadratic interpolation with three points was used.

The program proceeds as follows:

1. Extract segment of user-specified length from the overlapping segments of the lines in question.
2. Compute the complex one-dimensional FFT for both segments.
3. Compute the phase correlation function, $d = F^{-1} (G_1 \times G_2{}^*)/(|G_1| \times |G_2|)$ as an inverse FFT.
4. Find the maximum, d_n, and two adjacent values d_{n-1}, d_{n+1}.
5. Find the coefficients for the polynomial $h(x) = ax^2 + bx + c$ by interpolation through 3 points: $h(n - 1) = d_{n+1}, h(n)$ and $h(n + 1) = d_{n+1}$.
6. Find the offset as the maximum of the polynomial $L = -b/2a$.

Algorithm testing was performed on simulated image lines (Gaussian profiles shifted against each other) and on a Landsat TM line shifted against itself. In all cases the algorithm yielded expected shifts, i.e., the artificial shifts introduced a priori. Actual measures of band-to-band and line-to-line misregistration for selected TM scenes are displayed in Figures 1–5. The scales of the plots are exaggerated to reveal the low amount of actual misregistration recorded. It should be noted that mismatches in correlation sometimes occurred because of the variation in scene pattern between different bands or because the algorithm correlated on adjacent patterns (e.g., parallel roads).

Intraband Integrity. A test was developed to check a single band's geometric integrity on a mirror-scan swath basis. Band 3 (0.63–0.69) from each scene was chosen as the test case. To guarantee that swath edges were included, four lines in the vicinity of the presumed swath edges (multiples of 16 lines) were used in this test. It was verified that swath borders were included by examining the saw-tooth-like image edges on Scrounge products and computing swath positions on TIPS products.

It should be noted that the FFT method is scene dependent, which implies that interline differences are to be expected although their aggregate differences should be randomly dispersed along a line. The offsets of the adjacent lines were examined at 100 pixel spacings. The operational hypothesis was that correctly aligned swaths should result in small offsets randomly scattered and close to zero.

An analysis of the tabulated and plotted results revealed that line-to-line misregistration was in the order of 0.3 pixel maximum (Figure 1). Plots failed to show any systematic misregistration effects that can be directly associated with local jitter. These figures indicate that there are no apparent problems in the alignment of the corrected mirror scan swaths within a single band either for TM-4 Scrounge products or TM-5 TIPS products. Our findings are comparable to those of other Landsat-4 investigators. Band-to-band misregistration findings for this scene are essentially the same as those found by Barker (1983), Bender *et al.* (1983), Bernstein (1983), Card *et al.* (1983), and Gurney and Eng (1983).

Interband Registration. A similar test using the modified Kuglin and Hines method was performed to assess the interband registration of the high spatial resolution bands (i.e., all except band 6) of TM. Rather than looking at adjacent scanlines of one band, the same scanlines of different bands were taken to evaluate how closely they correlated. The assumption was made that although the bands were sensed in different spectral regions, their patterns would be similar for a given line of registered data. Systematic offsets in a certain direction (positive or negative) would be judged as misregistration between bands, whereas randomly variant (and small)
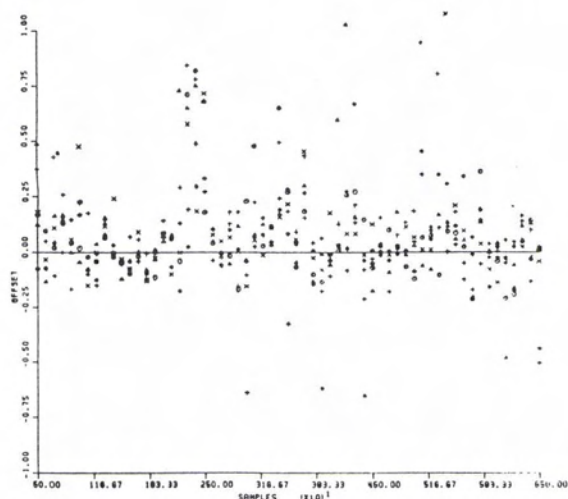
FIG. 1. Cumulative plot of registration offset of all line-to-line comparisons for lines 15 through 20 for band 3 of the Thematic Mapper scene 40109-15140, Washington, DC, 2 November 1982.
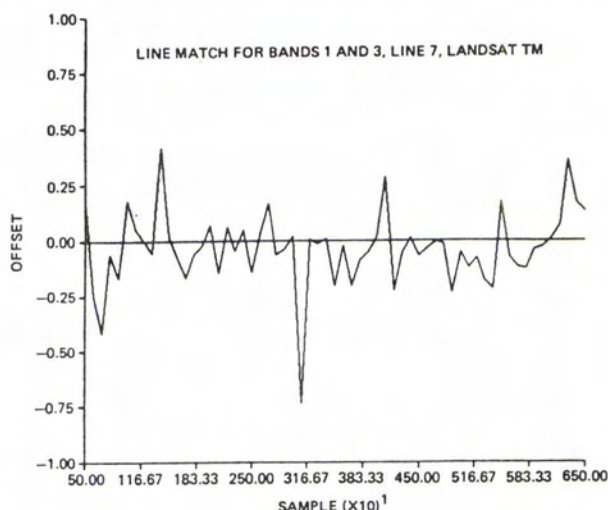
FIG. 2. Interband linematch correlation between bands 1 and 3 (both primary focal plane) for line 7 of Harrisburg, PA, Thematic Mapper P-Tape, Scene 40190-15134, 2 November 1982.

offsets would be indicative of well-registered data sets. It should be noted that mismatches in correlation sometimes occurred between different bands because of normal variation in scene patterns or anomalous features.

For the Landsat-4 TM, both A-data and P-data imagery for the Washington, DC, Harrisburg, PA, and Salton Sea, CA were examined. The results of the tests showed little systematic misregistration in the A or P data between bands of the primary focal plane (PFP) (bands 1–4). A typical plot of offsets between primary focal plane bands is presented in Figure 2. In these, misregistration varied between ±0.265 pixels 96 percent of the time and most frequently was within the ±0.15 pixel-offset range. No trends in pixel offsets were observed. Between bands of the primary focal plane and those of the secondary focal plane (SFP) (bands 5 and 7), pixel offsets were consistently negative and often in the range between −0.75 and −1.25 pixels for P-data. Figure 3 is a plot of offsets between bands of different focal planes. In this case and overall, the misregistration of the A-data was similar to that of the P-data. One significant difference between the two was the much improved registration between the high-resolution bands (bands 5 and 7) of the secondary focal plane in the P-data over the registration of the A-data (Figure 4). Thus, aside from problems between bands of different focal planes, the interband integrity of the P-data was within specifications. The A-data had similar characteristics, with unexpected misregistration between bands 5 and 7 of the secondary focal plane.

For the Landsat-5 TM, only the Washington, DC, and northwest Iowa scenes of P-data only were investigated. Bands 1 through 4, all in the PFP, appeared to be well registered with one another. Offsets determined by the correlation technique were both positive and negative and were randomly distributed about zero (Figures 5 and 6). Between bands 1 (PFP) and 5 (SFP), however, in both TM-
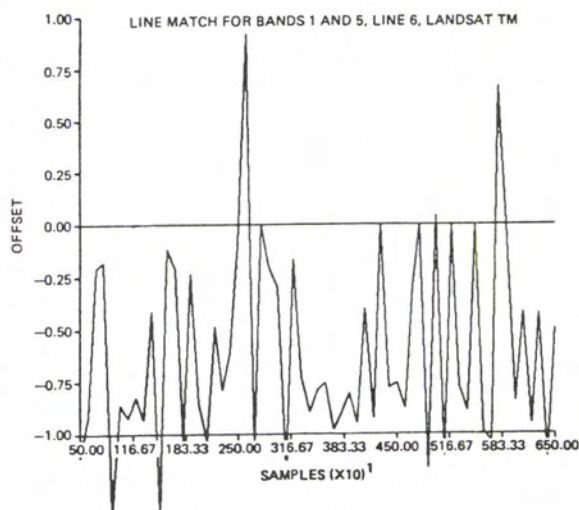
FIG. 3. Interband linematch correlation between bands 1 (primary focal plane) and 5 (secondary focal plane) for Harrisburg, PA, Thematic Mapper P-Tape, scene 40190-15134, 2 November 1982.
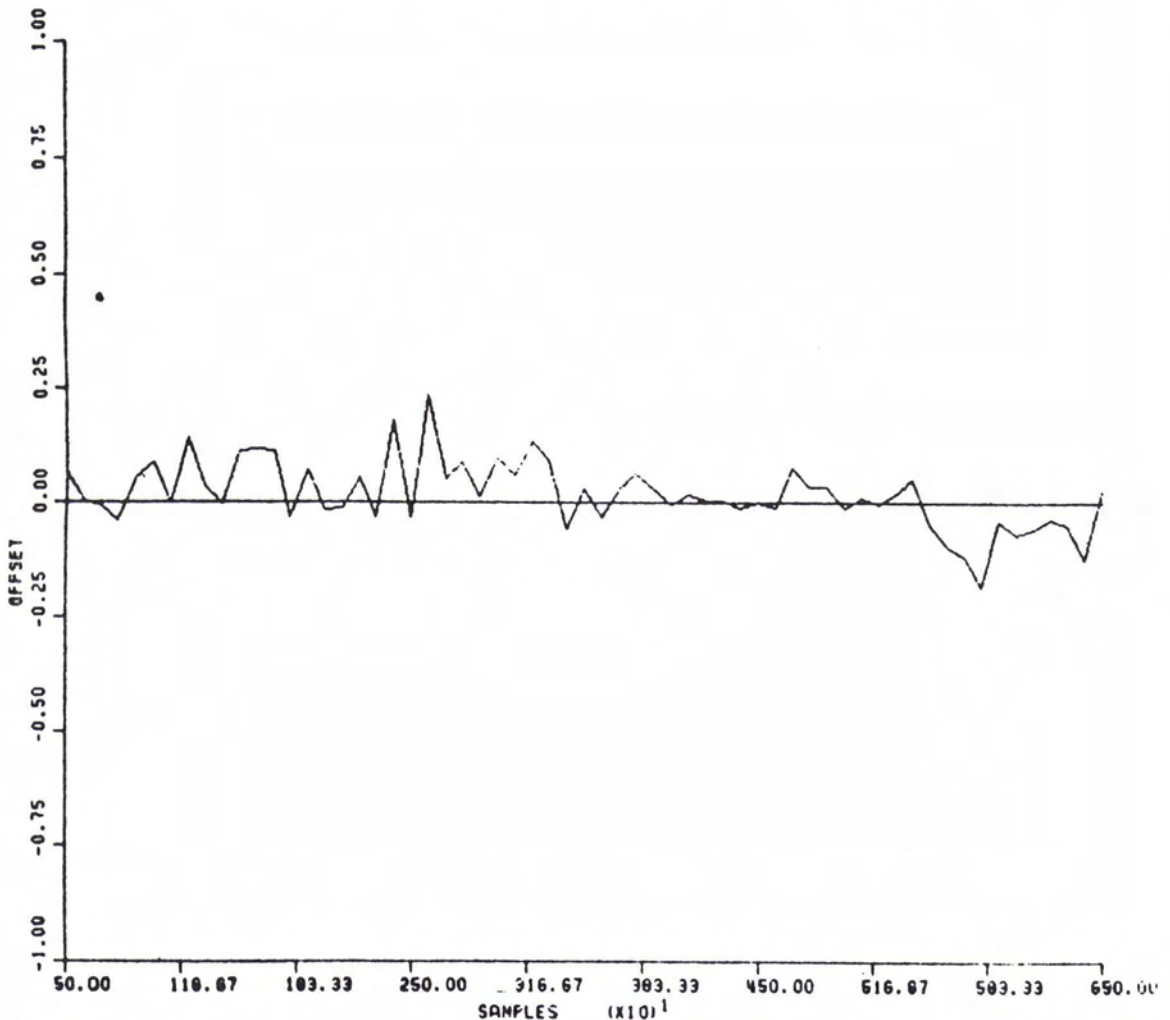
FIG. 4.   Band-to-band registration (5 vs. 7) for the cold focal plane of the Thematic Mapper along line 7 of scene 40109-15140, Washington, DC, 2 November 1982.

5 scenes analyzed, 85 to 90 percent of all offsets were negative, indicating a strong probability of systematic misregistration between those bands (Figure 7). The offsets were generally of small magnitude (i.e., <0 and ≥ -0.35 pixel). Questionably large offsets occurred between band 7 and all other bands in both the PFP and the SFP. They were so large that they are probably a result of either a failure in the correlation technique or a large dissimilarity of spectral reflectances between band 7 and all other bands for the areas examined.

IMAGE-TO-IMAGE CONFORMITY

A third part of this investigation concerned the conformity of P-tapes from the TIPS processed TM-5 data to the Scrounge processed TM-4 data. To test for such conformity, approximately 80 ground control points (GCP) were obtained for each of the TM-

4 scenes. The Iowa scene GCPs were collected by the USGS facility at Flagstaff, AZ. Those in the Washington, DC, scene came from points found previously at JPL. It should be noted that another test of image-to-image conformity could have been undertaken if two acquisitions for the same path/row from the same Landsat using ground control points had been available.

The procedure used in comparing the scene pairs involved using an algorithm which performs automated two-dimensional image correlations. Three independently established tiepoints between each scene pair were found, and based upon these tiepoint pairs, the routine computed a model transformation between the scenes. The line-sample coordinates of the input (TM-4) were transformed into predicted output coordinates in TM-5. The algorithm then computed the two-dimensional correla-
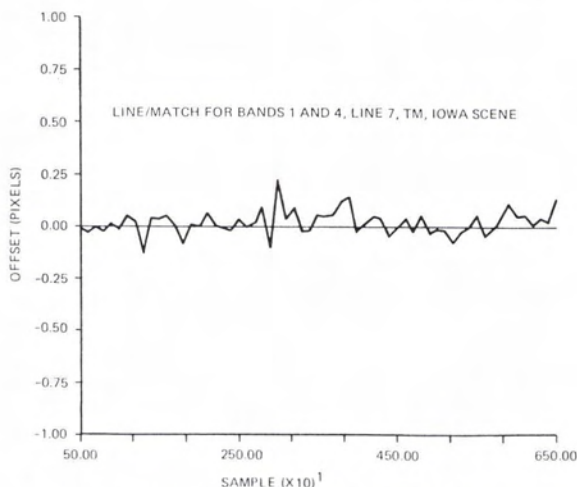
FIG. 5. Between band linematch correlation between two bands of the primary focal plane (PFP), in this case between bands 1 and 4, for northwest Iowa scene 50046-16324, 16 April 1984.
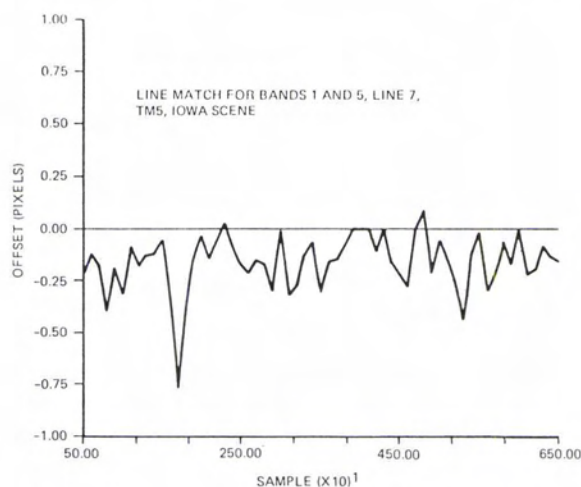
FIG. 7. Between band linematch correlation between band 1 (PFP) and band 5 (secondary focal plane) for Iowa scene 50046-16324, 16 April 1984.

tion function on a 64 × 64 pixel area surrounding the predicted point, and by finding its maximum, determined the point in the TM-5 data set which best corresponded to the input TM-4 tiepoint. Along with each best-fit point in TM-5 data, the algorithm computed the value of a correlation function which indicated how well the output point chosen actually fit the input TM-4 GCP. Due to changes in relative spectral characteristics of some areas, the algorithm failed to locate some of the points at or above the threshold correlation value. These points were discarded from further analysis. The routine was rerun with only the well-matching

points. The conformity of the TM-5 scenes to their TM-4 counterparts was reduced to linear equations describing the affine transformation from TM-4 to TM-5 scene. For Iowa:

$$
\begin{aligned}
\text{(TM-5 line)} = \ & 1.0001346 * \text{(TM-4 line)} \\
& + 0.000976 * \text{(TM-4 sample)} \\
& - 54.83 \qquad\qquad\qquad (3)
\end{aligned}
$$

$$
\begin{aligned}
\text{(TM-5 sample)} = \ & 0.000828 * \text{(TM-4 line)} \\
& + 1.0001051 * \text{(TM-4 sample)} \\
& + 109.8 \qquad\qquad\qquad (4)
\end{aligned}
$$

The coefficients of these equations indicate very little scene rotation and aspect distortion.

Analysis of the Washington, DC, scene yielded similar results. In general, the algorithm located points in the TM-5 scene which deviated only slightly from the point predicted by the initial model based upon the three tiepoints. These fits indicate an undistorted geometric correspondence between the Scrounge processed data and the TIPS processed image. They also indicate that after computing offset, scene to scene registration at the subpixel level should be achieved for areas the size of a TM quadrant or less in regions of low topographic relief.

CONFORMANCE TO GROUND CONTROL

Technique. The sensor and spacecraft geometric calibration analysis was checked using existing software and procedures recently developed at JPL (Zobrist *et al.*, 1983). Those procedures developed for mosaicking Landsat MSS scenes, were used to identify the offset from a least squares surface plane projected through ground control points located in the TM images, and on 1:24,000 and/or 1:62,500 topographic maps. Only those points which could
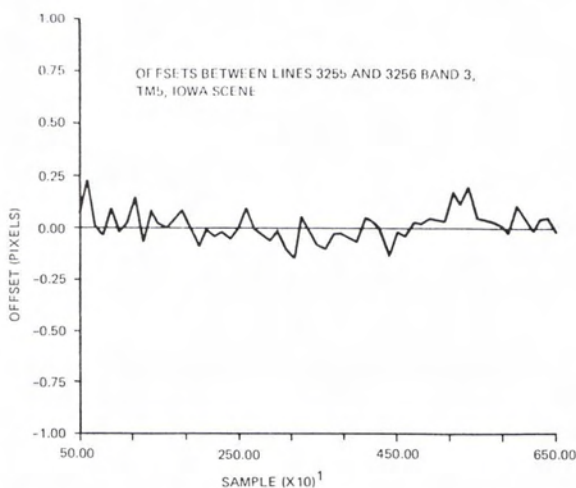
FIG. 6. Plot showing offsets between a swatch of a forward and a swath of a reverse scan in TM band 3, for northwest Iowa scene 50046-16324, 16 April 1984.

be precisely located on both the CRT and a map were selected. The GCP Earth coordinates were digitized from the maps with the dominant measurement error being a roundoff down to the nearest 1/10,000 of a degree. The next step was to compute the linear least-squares fit between the earth and image coordinate systems. This could not be done with a straightforward linear function because the TM data had been processed into a unique map projection called the Space Oblique Mercator (SOM).

The SOM Projection. An a priori knowledge of a satellite image's projection is essential in order to assess its conformity to Earth-surface geometry. Without its consideration, projection-induced deformations can result in trends of 'errors' of such magnitude that real sensor or processing errors are effectively obscured.

The standard projection in which Thematic Mapper data are processed, the SOM, was conceptualized by Colvocoresses (1974), and mathematically derived by Snyder (1978) and Junkins (1978) working independently. The SOM requires minimal pixel resampling and consequently reduced computer processing time, both of which are very important considerations in the handling of the immense data load of TM. Until recently, software which projects Earth coordinates into SOM coordinates (and the reverse) has not been available. One of the key steps in this research was the acquisition and implementation of the newly-developed SOM software from John Snyder at the National Cartographic Information Center (NCIC).

Before the SOM software was acquired, a preliminary linear least-squares fit between the unprojected Earth coordinates and the image coordinates was computed in order to better understand the SOM projection and its effects on image geometry. The mean residuals were close to 10 pixels (300 m), and their standard deviations were near 6 pixels (180 m). The residual vectors, plotted in two dimensions, produced systematic patterns which were attributable in part to the SOM projection (not shown here).

The Least-Squares Fit. The SOM software, once received, was put into an Image Based Information System (IBIS)* routine through which the Earth coordinates were projected into their SOM equivalents. A linear least-squares fit was then performed on the TM-4 Harrisburg and Salton Sea scenes using the SOM coordinates as the independent variables (since the map accuracies were known) and the

---

* The Image Based Information System (IBIS) is a computer-based system enabling the analysis of a variety of phenomena in a geographic context. As a subset of the VICAR (Video Image Communication and Retrieval) processing system, it allows for the vector and tabular as well as raster data-type inputs (Bryant and Zobrist, 1976).

image coordinates as dependent variables. Both coordinates were input in terms of meters. The parameters of the linear fit (which related the TM image to absolute locations on Earth) were not studied, since the early ground processing of TM data did not utilize ground data references to accurately locate absolute position.

On the first run a few of the GCPs had unreasonably large residuals. Consequently, those GCPs were removed from the analysis. In the edited data the resulting residuals were quite small: for the Salton Sea scene the mean of the 165 residuals was 40.46 m (1.35 pixels) with a standard deviation of 30.57 m (1.02 pixels). The Harrisburg scene residuals were smaller, with a mean of 28.38 m (0.95 pixels) and a standard deviation of 19.82 m (0.66 pixels) for the 219 GCPs examined. Two-dimensional plots of the residual vectors, magnified by a factor of 60 to enhance visibility, are presented for both the Harrisburg and the Salton Sea scenes in Figures 8 and 9. No significant trends were detectable in the two-dimensional plots of the residuals. The maximum offset for the smallest 90 percent of the residuals was 70.37 m (2.35 pixels) for the Salton Sea scene and 52.78 m (1.76 pixels) for that of Harrisburg. These results are similar to those found by Wrigley *et al.* (1984) and Welch and Usery (1984).

CONFORMANCE OF IMAGE PROJECTIONS TO MAPPED PROJECTIONS

With the decreasing IFOVs of satellite sensors, the closeness of approximation of GCP locations has become a crucial factor in the assessment of data geometric properties. Chi-square tests of confidence in the geometric conformity of the TM-4 Harrisburg and Salton Sea scenes and the northwest Iowa TM-5 scene were undertaken. The TM-5 TIPS product analysis is reviewed here:

SOM Error Budget. The error specified for the TIPS product was one-half of a pixel 90 percent of the time. This meant that the SOM-projected pixels should be within 15 m of where they would be in a perfect SOM map of the area. Note that this is an accumulated system error bound including all errors prior to TIPS processing.

The method is to find ground control points (GCPs) on 1:24,000 maps in latitude/longitude coordinates. Applying the SOM transformation on these yields a SOM coordinate position which may still be off by a linear transformation from the SOM-projected Landsat. (This is a general linear transformation that includes slides, rotates, and skews.) The statistical assumption that the transformation is linear is tested by performing linear regression and calculating chi-squared for the residuals:

$$\chi^2 = \frac{1}{n-2} \sum_{i=1}^{n} \frac{e_i^2}{\sigma_i^2} \qquad (5)$$

FIG. 8.   Two-dimensional plot of residuals between GCP line-samples and SOM XYs for Harrisburg, PA, Thematic Mapper scene 40109-15134, 2 November 1982 (magnification factor 60).

where e_i is the residual error reported for the ith GCP in the SOM projected image and σ_i is the root mean square measurement error in e_i.

The northwest Iowa scene was used for this test. Fifty GCPs were chosen from 1:24,000 paper maps of the area, and the corresponding line-sample locations were identified by cursor (a computerized cross-hair) on an image display screen with enlargement capability. The map latitudes/longitudes were converted to SOM coordinates using a computer routine with negligible error. A least-squares linear fit of the SOM coordinates to the pixels' locations was performed with negligible error. The resulting residual error was 31.4 m RMSE. Thus,

$$\chi^2 = \frac{N}{N-2} \cdot \frac{\text{mean (residual}^2)}{\sigma^2} \qquad (6)$$

Table 2 shows an allocated error budget for calculating σ. The TIPS processing error is included, and is reduced from the 90 percent fraction to a one sigma error distance. The resulting χ^2 is 1.906 which gives weak confidence that the TIPS product is linearly related to an SOM map of the Earth's surface.

The next step is to enlarge the TIPS error bound to bring χ^2 below 1.0 which would correspond to a confidence level of 0.5 that the TIPS product met its error bound. By allowing the TIPS RMSE to be 23.89 m a χ^2 of 1.0 results. This corresponds to an error of 39.5 m or less, 90 percent of the time, or about one and one-third pixels.

Referring to Figure 10, note that most of the GCPs were chosen around the perimeter of the Iowa scene, so the statistical test was rather stringent.
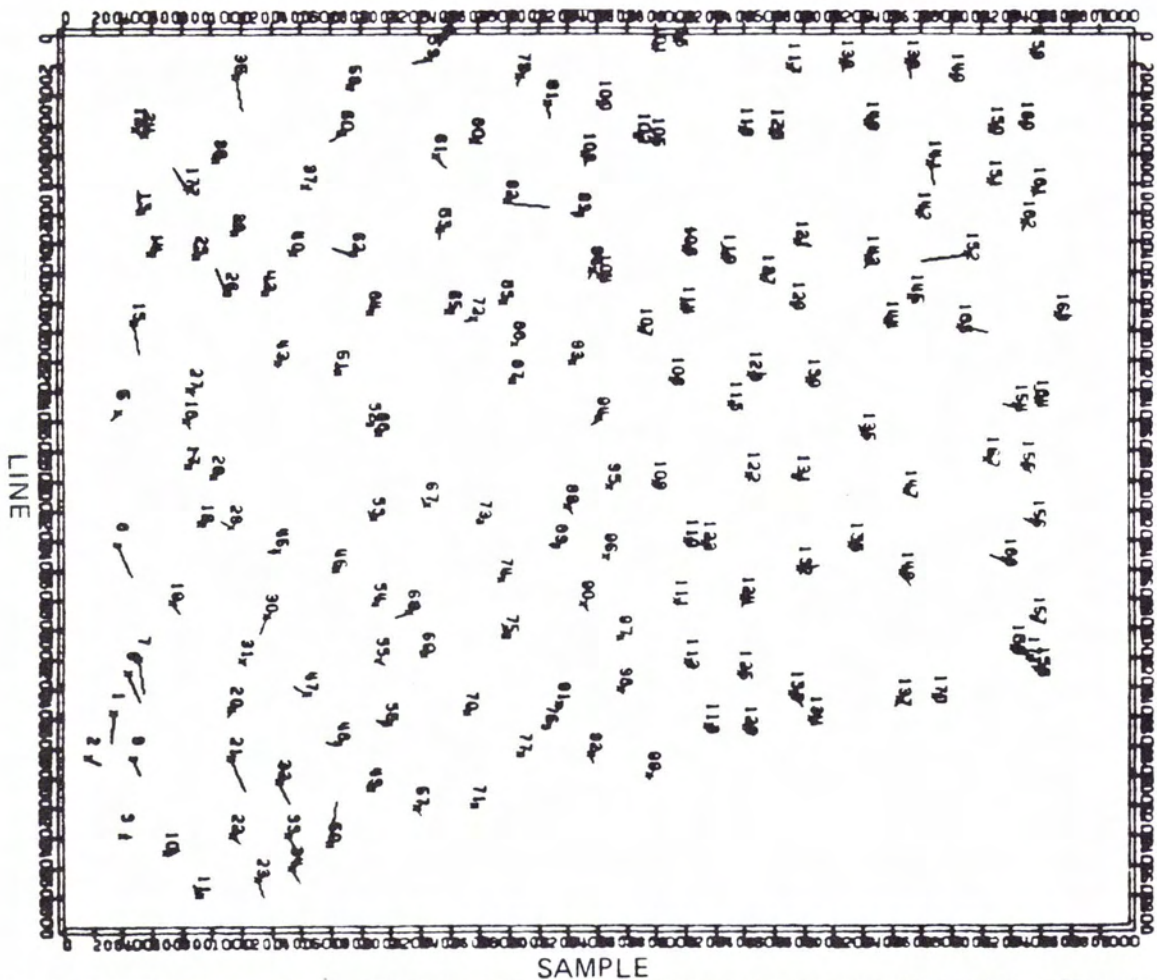
FIG. 9. Two-dimensional plot of residuals for Salton Sea, CA, Thematic Mapper scene 40149-17444, 12 December 1982.

Spacecraft Ephemeris and the SOM Projection. The lack of conformity of the SOM projected latitude/longitude position of a ground control point (GCP) and the observed position of that GCP revealed by the chi-squared goodness of fit test initiated a search for the cause. It was first noted that the SOM uses the centerpoint for a given frame and the center pixel for the first and last line in a scene to compute a unique projective geometry for that scene and that scene alone. The centerpoint pixel determines the northing from the equator, and the center pixels of the first and last scene determine the prime meridian orientation (see Synder, 1978). This point is illustrated in Figure 11, which maps the exaggerated vector offsets between a SOM projected version and UTM projected version of the Landsat-5 Harrisburg scene where ground control points were used. It can be seen from the figure that the distortion surface is not affine, but rather a complex polynomial that can only be recovered by the selection of a number of GCPs. Conversely, the development of a correct SOM projection depends on an accurate assignment of latitude and longitude to the centerpoint of a scene, and any deviation from absolute positioning knowledge will incur projection distortions recoverable only by the selection of a

TABLE 2. ERROR BUDGET FOR CHI-SQUARED TEST OF SOM PROJECTED TM IMAGE TO EARTH'S GEOMETRY SCENE 50046-16324 (ELEVATION EXCLUDED)

	Pixels (RMS)	Meters (RMS)
TIPS Specified Error	0.302	9.07
GCP Location in Image	0.670	20.00
Map Accuracy (1:24,000)	0.250	7.50
		23.21
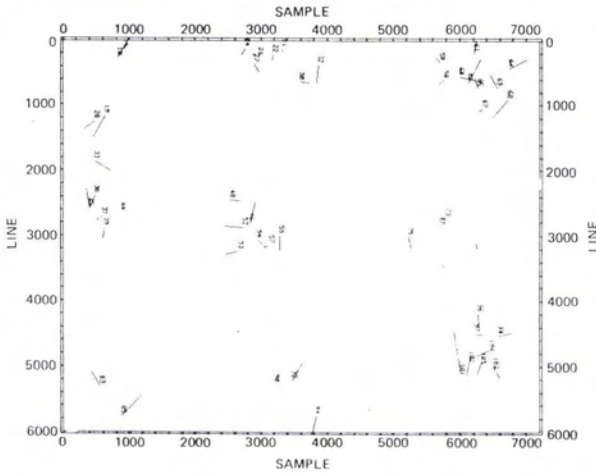
FIG. 10. Two-dimensional plot of residuals between GCPs found in TM-5 northwest Iowa scene (50046-16324) 16 April 1984 and SOM projected latitudes/longitudes of the same (magnification factor 300).

number of GCPs and the development of a complex polynomial surface.

The accuracy of the SOM for any scene is only as good as the orbit ephemeris data. The ephemeris constraints, as specified in the Landsat Ground Station Interface Description (1984), are rigorous, but

not rigorous enough to enable the SOM to be used without ground control or the Global Positioning System (GPS) to obtain the actual nadir track and scene centerpoint positions. Table 3 summarizes these findings for selected TM-5 scenes. Avoidance of this problem for the SOM projection can be achieved if the TIPS processing segment were systematically to receive a more accurate ephemeris by using the GPS or identifying a select number of ground control points along an orbit swath.

Further investigations showed that another alternative exists if the TM data are projected in the UTM projection. The UTM projection has a designated prime meridian within a zone rather than the SOM choice of the nadir track as a prime meridian. Because of this fact, when the TM ephemeris is calculated in the absence of ground control, but projected in UTM, any discrepancy is the function of a northing and easting offset. Figure 12, which displays the vector offsets for the Landsat-5 Des Moines, IA, scene projected to UTM (one with and one without ground control) illustrates this point. The vectors, all uniform, represent the actual versus observed centerpoint difference of 54.339 m easting and 279.772 m northing. Thus, the user can avoid any need to apply complex polynomial surface fits to data sets to be registered to a TM scene if the UTM projection (*not* the default option) is specified, and three or more GCPs are used to calculate an offset correction to apply to the nominal header information.

CONCLUSIONS

The results of this investigation indicated that Thematic Mapper imagery, in terms of geometry, has come close to, and in some cases exceeded, its stringent specifications. Single bands appeared to have properly aligned forward and reverse scans in the corrected P-data, and interband registration, ac-
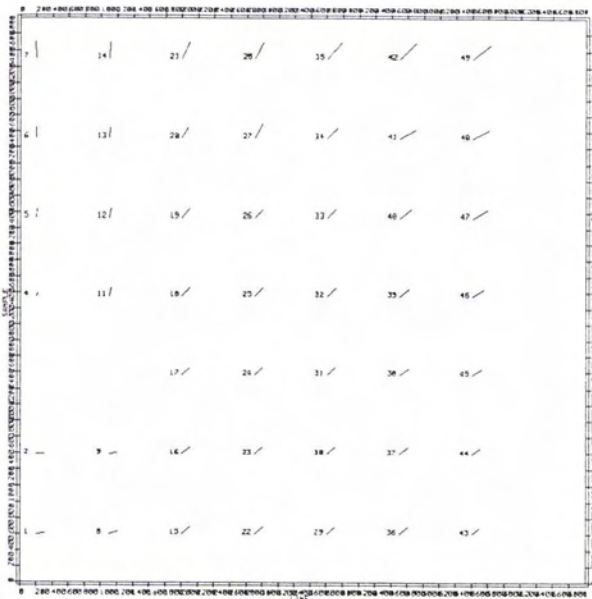
FIG. 11. Two-dimensional plot of vector offsets between SOM and UTM projections of TM-5 scene (50099-15141) of Harrisburg, PA, dated 8 June 1984. Both scenes had TIPS processing with GCPs. Offsets reflect difference between UTM zonal and SOM scene specific projective geometries.

TABLE 3. CENTERPOINT LOCATION OF TM-5 P-TAPE SCENES CALCULATED FROM EPHEMERIS VERSUS OBSERVED FROM GROUND CONTROL

	Northwest Iowa (50046-16324) SOM	Des Moines, IA (50114-16223) UTM
Ephemeris Calculated:		
Northing (km)	608.9104	4,623.8701766
Easting (km)	15,266.3305	499.5803424
Ground Control Point Observed:		
Northing (km)	607.8507	4,623.8647427
Easting (km)	15,266.0477	499.5523652
Difference:		
Northing (km)	1,059.7000	54.3390000
Easting (km)	282.5000	279.7720000
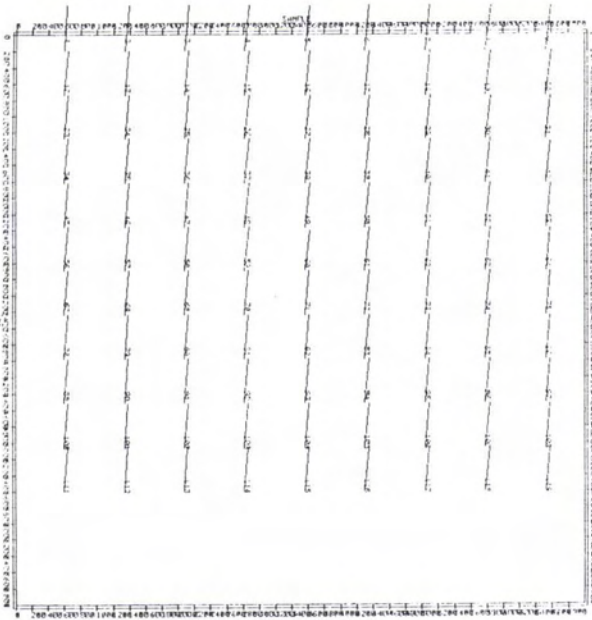
FIG. 12.   Two-dimensional plot of vector offsets between TIPS processed TM-5 imagery of Des Moines, Iowa scene 850114-16223) dated 23 July 1984, one with and the other without GCPs.

cording to the methods used, was well within the required tolerances. The overall geometric quality of P-data was very good. The SOM-projected Earth coordinates left small residuals when fitted to the image coordinates with a linear least-squares function in the scenes scrutinized. The budgeted RMS errors were close to the mean residuals; thus the fit might very well have been better than the results indicated.

The TM data were highly accurate to the UTM projection and good for SOM over the entire scenes. The absolute locations were unknown for early scenes due to the lack of geodetic control in the Scrounge ground processing system. For these scenes users must find three or more points to establish a georeference for the whole scene. Users are advised to obtain the SOM projection software from NCIC to locate within or process the scene. Polynomial fitting to GCPs is not recommended for relating TM data to other geographic coordinate systems, as low-order polynomials do not fit TM well and higher order polynomials exhibit bad behavior in the corners of the scene.

The absolute projective geometry for TM scenes without ground control exceeds the limits of the chi-squared goodness of fit criteria when SOM projections are applied. This is a function of the SOM projection characteristics, and can easily be avoided by specifying UTM projected products, observing the absolute offset, and applying it to the scene.

REFERENCES

Barker, J. L., 1983. TM Report, paper presented at the Landsat-4 Early Results Symposium: GSFC, Greenbelt, MD, February 22-24.

Bender, L. U., et al., 1983. An Evaluation of Landsat-4 Thematic Mapper Data for Their Geometric and Radiometric Accuracies and Their Relevance to Geologic Mapping: paper presented at the Landsat-4 Early Results Symposium, GSFC, Greenbelt, MD, February 22-24.

Bernstein, R., 1983. An Analysis and Evaluation of the Landsat-4 MSS and TM Sensors and Ground Data Processing System—Early Results: paper presented at the Landsat-4 Early Results Symposium, GSFC, Greenbelt, MD, February 22-24.

————, 1973. Scene Correction (Precision Processing) of ERTS Sensor Data Using Digital Image Processing Techniques: *Third Earth Resources Technology Satellite-1 Symposium*, Vol. 1, sec. B, pp. 1909-1927.

Beyer, E. P, 1981. Geometric Error Characterization and Error Budgets: (Landsat-D Thematic Mapper Processing), paper presented at NASA Workshop on Registration and Rectification, Leesburg, Virginia, November 17-19.

Billingsley, F. C., 1981. *Effects of Misregistration on the Accuracy of Multispectral Classification:* JPL Technical Memorandum 81-6, Pasadena, CA, April 15.

Bryant, N. A. and A. L. Zobrist, 1976. IBIS: A Geographic Information System Based on Digital Image Processing and Image Raster Datatype: *Proceedings of the LARS Symposium on Machine Processing of Remotely Sensed Data*, Lafayette, IN, June.

Card, D. H., et al., 1983. Assessment of Thematic Mapper Band to Band Registration by the Block Correlation Method: Preliminary Results, paper presented at the Landsat-4 Early Results Symposium, GSFC, Greenbelt, MD, February 22-24.

Colvocoresses, A. P., 1974. Space Oblique Mercator, A New Map Projection of the Earth . . . , *Photogrammetric Engineering*, v. 40, no. 8, pp. 921-926.

Graham, M. H. and Luebbe, 1981. An Evaluation of MSS P-format Data Registration," NASA paper N81-33557.

Gurney, C. and K. Eng, 1983. The Use of Linear Feature Detection to Investigate Thematic Mapper Data Performance and Processing, paper presented at the Landsat-4 Early Results Symposium, GSFC, Greenbelt, MD, February 22-24.

Junkins, J. L. and J. D. Turner, 1977. Formulation of a Space Oblique Mercator Projection, Final Report No. UVA/525023/ESS77/105, Computer Science Laboratory, U.S. Army ETL, November.

Landsat Ground Station Interface Description, GSFC 435-D-400, Rev. 8, June 1984, Table 1, p 6.

Kuglin, C. D. and D. C. Hines, 1977. The Phase Correlation Image Alignment Method, SPIE, *Application of Digital Image Processing*, Vol. 119, (IOCC 1977).

Prakash, A. and E. P. Beyer, 1981. Landsat-D Thematic Mapper Image Resampling for Scan Geometry Correction, *1981 Machine Processing Remotely Sensed Data Symposium*, LARS, Purdue University, 11 pp.

Snyder, J. P., 1978. The Space Oblique Mercator Projection, *Photogrammetric Engineering and Remote Sensing*, v. 44, no. 5, pp. 585-596.

Welch, R. and E. L. Usery, 1984. Cartographic Accuracy of Landsat 4 MSS and TM Image Data, *IEEE Transactions on Geoscience and Remote Sensing*, v. GE-22, no. 3, (May), pp. 281-287.

Wrigley, R. C., et al., 1984. Thematic Mapper Image Quality: Registration, Noise, and Resolution, *IEEE Transactions on Geoscience and Remote Sensing*, Vol. GE-22, No. 3, (May), pp. 263-271.

Zobrist, A. L., Bryant, N. A., and McLeod, R. G., 1983. Technology for Large Digital Mosaics of Landsat Data: *Photogrammetric Engineering & Remote Sensing*, v. 49, no. 9 (Sept.), pp. 1324-1335.

Forthcoming Articles

Peter O. Adeniyi, Digital Analysis of Multitemporal Landsat Data for Land-Use/Land-Cover Classification in a Semi-Arid Area of Nigeria.

Paul S. Anderson, Millimetric Coordinates (MMC): Communication and Teaching Aid.

M. L. Benson, B. J. Myers, I. E. Craig, and *W. C. L. Gabriel*, A Practical Field Stereo Viewer for 230-mm Color Transparencies.

Steven L. Birge, Highway Dimensions from Photolog.

W. T. Borgeson, R. M. Batson, and *H. H. Kieffer*, Geometric Accuracy of Landsat-4 and Landsat-5 Thematic Mapper Images.

D. E. Bowker, Priorities for Worldwide Remote Sensing of Agricultural Crops.

James K. Crossfield, A High Precision Photogrammetry Geodetic Positioning Cost Model.

S. Curry, J. M. Anderson, S. Baumrind, and *B. Wand*, Stereo Camera and Stereo X-Ray Devices: Comparison of Biostereometric Measurements.

J. L. Davidson, Stereo Photogrammetry in Geotechnical Engineering Research.

S. F. El-Hakim, Photogrammetric Measurement of Microwave Antennae.

J. H. Everitt and *P. R. Nixon*, Using Color Aerial Photography to Detect Camphorweed Infestations on South Texas Rangelands.

Gary E. Ford and *Claudio I. Zanelli*, Analysis and Quantification of Errors in the Geometric Correction of Satellite Images.

Lawrence Fox III, John A. Brockhaus, and *Nancy D. Tosta*, Classification of Timberland Productivity in Northwestern California Using Landsat, Topographic, and Ecological Data.

Clive S. Fraser, Photogrammetric Measurement of Thermal Deformation of a Large Process Compressor.

W. Frobin and *E. Hierholzer*, Simplified Rasterstereography Using a Metric Camera.

John N. Hatzopoulos, An Analytical System for Close-Range Photogrammetry.

V. Kratky, Software Simulation of On-Line Analytical Systems.

G. D. Lodwick and *S. H. Paine*, A Digital Elevation Model of the Barnes Ice-Cap Derived from Landsat MSS Data.

Fred C. Martin, Using a Geographic Information System for Forest Land Mapping and Management.

Haim B. Papo, Deformation Analysis by Close-Range Photogrammetry.

A. J. Richardson, R. M. Menges, and *P. R. Nixon*, Distinguishing Weed from Crop Plants Using Video Remote Sensing.

William J. Ripple, Asymptotic Reflectance Characteristics of Grass Vegetation.

Robert A. Ryerson, Richard N. Dobbins, and *Christian Thibault*, Timely Crop Area Estimates from Landsat.

Alain Royer, Pierre Vincent, and *Ferdinand Bonn*, Evaluation and Correction of Viewing Angle Effects on Satellite Measurements of Bidirectional Reflectance.

Gerry Salsig, Calibrating Stereo Plotter Encoders.

Patricia A. Schultejann, Structural Trends in Borrego Valley, California: Interpretations from SIR-A and SEASAT SAR.

S. S. Shen, G. D. Badhwar, and *J. G. Carnes*, Separability of Boreal Forest Species in the Lake Jennette Area, Minnesota.

C. Dean Tritch, Is Your Contact Printer *Really* a "Contact" Printer.

John F. Watkins and *Hazel A. Morrow-Jones*, Small Area Population Estimates Using Aerial Photography.

T. H. Lee Williams, Implementing LESA on a Geographic Information System—A Case Study.